N65-81111
Code None
(NASA CR-52196)

SOCIETY OF AUTOMOTIVE ENGINEERS, INC.
485 Lexington Avenue, New York 17, N. Y.

Considerations in Design of Calorimeters for the Project FIRE Superorbital Re-Entry Test Vehicle

F. D. Linzer and Eli Kaplan
Republic Aviation Corp.

[1963]

Presented at the

SOCIETY OF AUTOMOTIVE ENGINEERS

National Aeronautic and Space Engineering and Manufacturing Meeting,
Los Angeles, Calif.
Sept. 23-27, 1963

750L

(NASA Contract NAS1-196

2496003
Republic Aviation Corp., Farmingdale, N.Y.

Considerations in Design of Calorimeters for the Project FIRE Superorbital Re-Entry Test Vehicle

F. D. Linzer and Eli Kaplan
Republic Aviation Corp.

The United States space program includes plans to safely recover lunar and interplanetary probes and manned lunar exploratory craft within the next decade. A major problem exists in designing such vehicles to withstand the rigorous thermal environment to which they will be subjected during re-entry into the earth's atmosphere at superorbital speeds. Under these conditions heat fluxes to the vehicle surfaces will far exceed those experienced during ICBM and satellite re-entries. To date, neither laboratory nor analytical techniques are sufficiently advanced to permit a high degree of confidence in the quantitative prediction of heat transfer in the hyperbolic re-entry flight regime.

Project FIRE, sponsored by the NASA Langley Research Center, is an experimental program to obtain actual flight data at a re-entry velocity of 37,000 ft/sec. This velocity is characteristic of a returning lunar exploratory craft such as Apollo. Interplanetary probes re-entering at still higher velocities may be the subject of later programs.

The work on which this paper is based was performed under contract to the National Aeronautics and Space Administration, Langley Research Center, Flight Re-Entry Programs Office, under Contract No. NAS 1-1945.

The Project FIRE re-entry test package under development by the Space Systems Division of the Republic Aviation Corporation is to be launched from the Atlantic Missile Range by an Atlas D booster. After launch and separation from the booster, the re-entry test package will coast for approximately thirty minutes after which time an Antares X-259 solid propellant rocket will ignite and accelerate the test package back into the atmosphere (Fig. 1). At the test

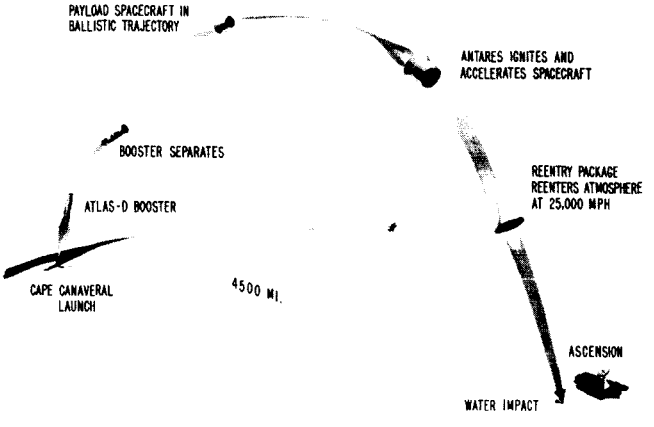

Fig. 1 - Project FIRE trajectory

ABSTRACT

16836

The purpose of Project FIRE and the nature of the re-entry package are briefly discussed. The function, location, and design of beryllium calorimeters for the forebody and gold calorimeters for the afterbody are described. Methods of achieving one-dimensional heat flow in the forebody calorimeter design are covered. For the afterbody calorimeter, the optimum design was determined to be a thermally isolated, small diameter, relatively thin disc of high thermal conductivity. The influence of thermocouple size, accuracy of thermocouple placement, heat losses, and other considerations are discussed in relation to accuracy of the sensor units. Derived equations are presented which may be used to convert the telemetered temperature responses into heat flux values.

AUTHOR

velocity of 37,000 ft/sec, the Antares rocket is separated from the re-entry test package and the latter commences the experimentally significant portion of the flight. The re-entry period lasts for approximately 40 seconds during which time heat transfer data will be telemetered to ground stations and simultaneously stored in a tape recorder aboard the vehicle. An ancillary objective of the experiment is to determine how successfully this information may be transmitted during the so-called "blackout" period. Retransmission of the data from the tape recorder will occur 45 seconds after initiation of re-entry, when the package is past the re-entry pulse, and normal radio communication may be resumed. This will ensure aquisition of the data should the "blackout" period telemetry prove inadequate. The package will not be recovered.

The re-entry test package is conical in shape similar to the Apollo vehicle, is approximately two feet in diameter, and weighs 185 pounds. It will re-enter blunt face foremost at zero angle of attack, and with a nominal entry angle of -14.7°. During the re-entry period, heat transfer to the vehicle will be measured at several points on the front face and afterbody as shown in Fig. 2.

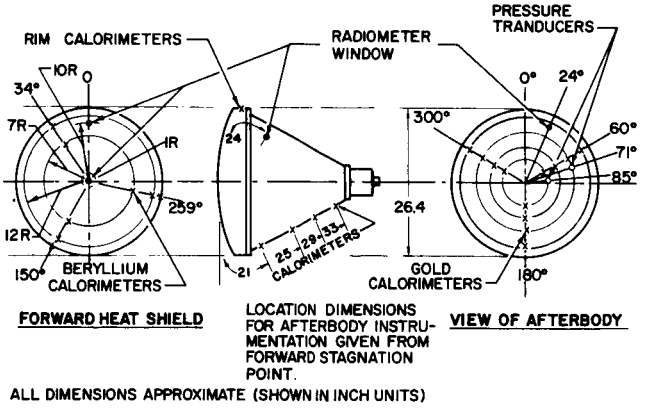

Fig. 2 - Calorimeter locations

The forward face of the vehicle will experience both convection from the boundary layer and radiative heat flux from the gas cap, while the afterbody heat input will be primarily convection from the boundary layer in a separated flow regime. Radiation heat flux from the gas cap to the forward face exists in equilibrium and non-equilibrium forms. Equilibrium radiation is generated throughout the gas cap (Ref. 1), while non-equilibrium radiation occurs in the region of the gas cap immediately behind the shock front. It is the non-equilibrium radiation that is the least understood to date, but recent laboratory experimental results (Ref. 2) have shown encouragingly good agreement with theoretical predictions.

Heat flux will be measured through application of calorimeters and radiometers. The calorimeters are on the vehicle surface and are essentially small metallic heat sinks that absorb the convective and a portion of the incident radiative heat flux. Internal thermocouples measure temperature-time histories of the calorimeter slugs, and thereby permit calculation of the heat flux versus time histories. Figure 2 shows the distribution of these calorimeter slugs which will determine the flux variation at different points on the vehicle.

Radiometers, viewing the flow field through quartz windows flush mounted on the vehicle surfaces, will measure spectral radiative flux from 2000 to 6000 Å at the stagnation point, total radiative flux at another point on the front face near the shoulder, and total radiation at a point on the afterbody. Through analysis of these measurements, the magnitude of radiation intensity will be determined.

The predicted convective and radiative fluxes at the stagnation point during re-entry and their summation are shown in Figs. 3 and 4. The predicted afterbody heat flux is shown in Fig. 5.

A basic requirement of the experiment is that the measurements be made in a contamination-free atmosphere where the flow field is not perturbed by gaseous products such as those resulting from an ablating heat shield. Contamination could materially influence the heat transfer and gas cap spectral radiation data, thus rendering the experimental results extremely questionable. There is, however, no

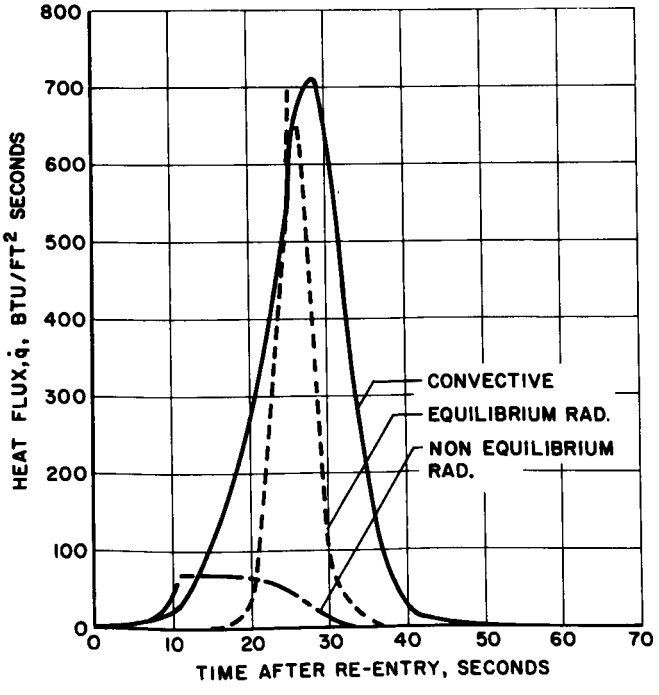

Fig. 3 - Stagnation region anticipated convective and radiative heat fluxes

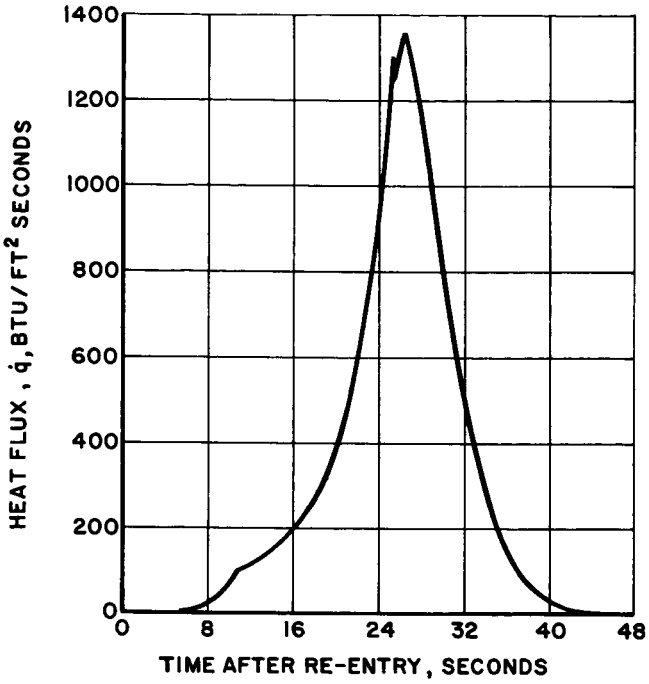

Fig. 4 - Stagnation region anticipated total re-entry heating flux

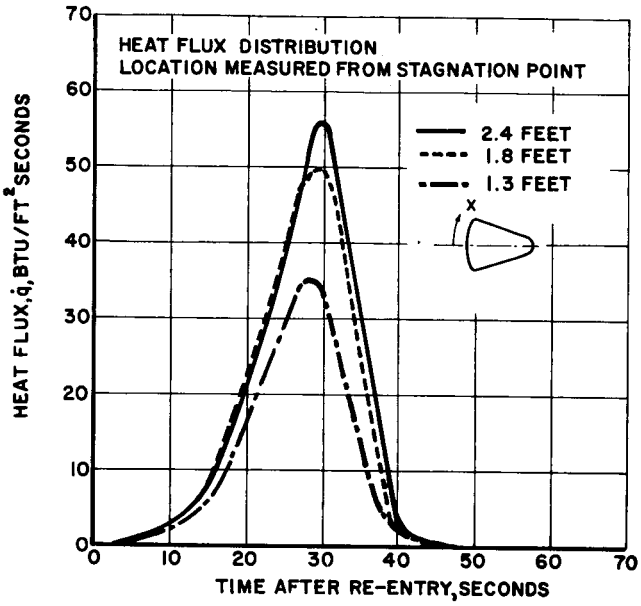

Fig. 5 - Afterbody anticipated re-entry heating flux (separated flow)

material available which can satisfactorily withstand the severity of the forward face heat pulse of Fig. 4 without ablating. It was, therefore, necessary to devise a means of utilizing a heat shield until it commences to ablate, discarding it, and replacing it with a fresh one that would provide an additional amount of "clean" experiment time. A pragmatic approach to this problem was taken by fabricating a three-layer heat shield as shown in Fig. 6. The first and third beryllium layers are 0.12 inches thick, and the second is 0.20 inches thick. They are separated from each other by an 0.20-inch layer of phenolic asbestos. During the initial portion of re-entry the outermost shield is subjected to the rising heat flux of Fig. 4. Until melting begins, after 21 seconds, the calorimeters in this first beryllium shield gather meaningful heat flux data. Approximately 3.5 seconds later this beryllium layer is completely ablated away exposing the phenolic asbestos layer beneath. The insulation layer of phenolic asbestos then protects and prevents heating of the second beryllium shield behind it until the peak heating point is approached. At a preselected instant, an acceleration-time signal initiates ejection of the phenolic asbestos shield (Fig. 7), and exposes the second beryllium shield whose calorimeters gather valid data for approximately 2.5 seconds before the onset of melting. After melting is completed, the third beryllium shield is protected for a short time by the second phenolic asbestos layer until the latter is ejected to permit the third shield calorimeters to record heat flux during the final portion of the re-entry period. This system is the best practical approach for obtaining a maximum amount of usable data during the re-entry period. One inherent disadvantage of the system is that data of limited usefulness is obtained during the interval between onset of melting of each beryllium shield and ejection of its phenolic-asbestos back-up layer. However, proper timing of ejection ensures collection of usable data during the most significant portions of the re-entry period.

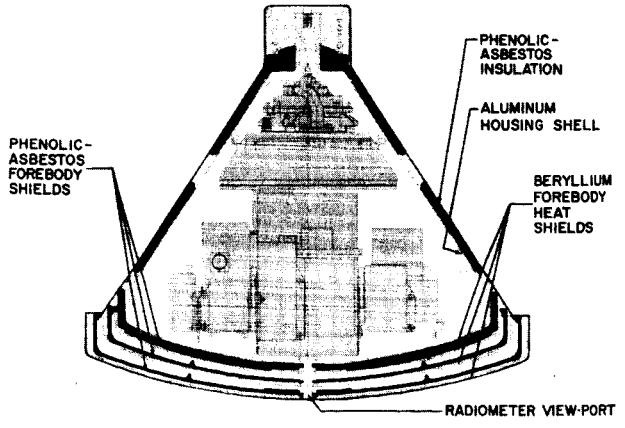

Fig. 6 - Re-entry test package cross section

The afterbody heat flux, as seen in Fig. 5, is only a small fraction of that experienced on the forward face. There is no need for a "layered" arrangement here and the afterbody

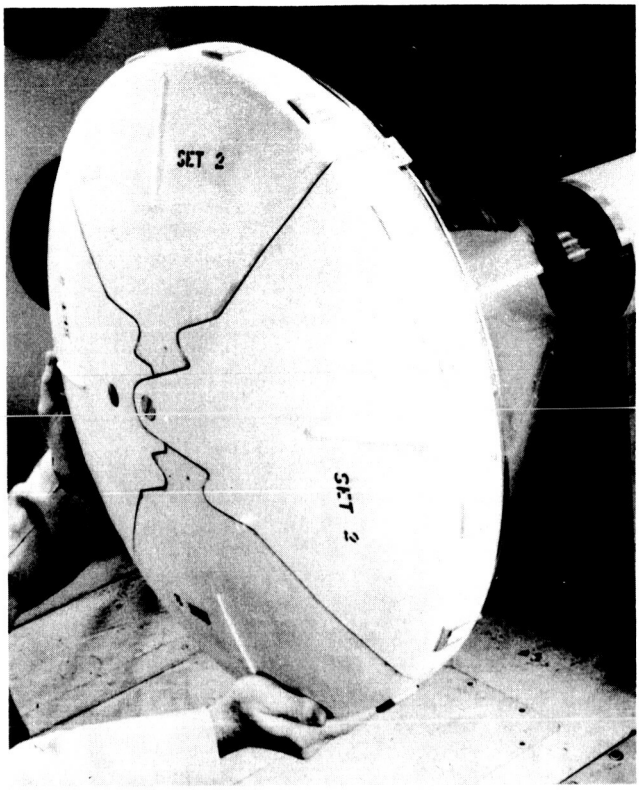

Fig. 7 - Phenolic asbestos forebody heat shield

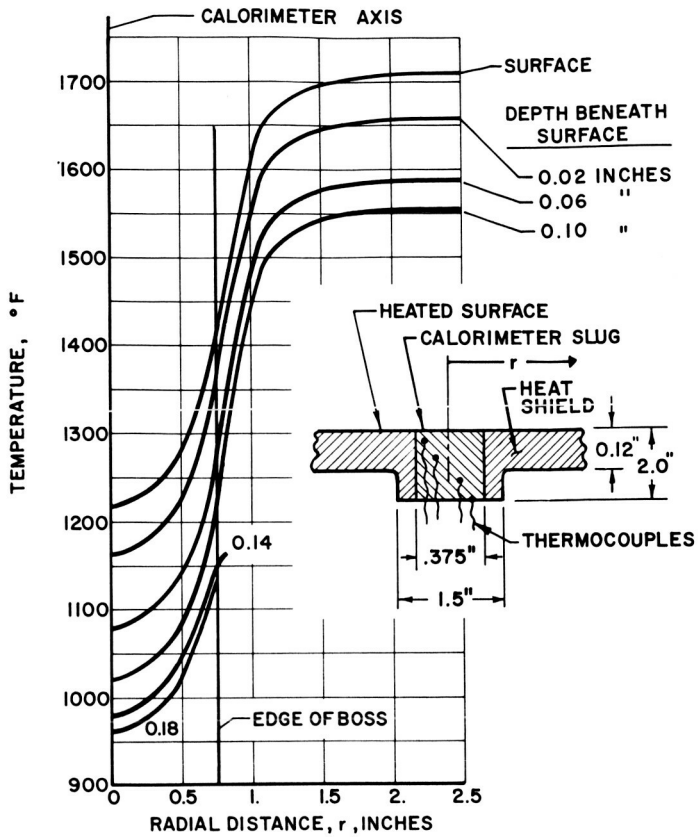

Fig. 8 - Instantaneous time-temperature pattern on first beryllium heat shield boss (1.5-inch diameter calorimeter boss)

calorimeters will provide a continuous heat flux reading throughout re-entry without melting.

It is the purpose of this paper to discuss the various considerations that entered into the design of the forebody and afterbody calorimeters.

FOREBODY CALORIMETERS

The three beryllium heat shields each contain 12 cylindrical calorimeter slug assemblies. These calorimeters, manufactured by the High Temperature Instruments Company of Philadelphia, Pennsylvania, are machined from the same material batch as the beryllium heat shields into which they are shrink fitted. The slugs are furnished with four thermocouples located at different depths. These are shown schematically on the cross-sectional insert sketches of Figs. 8 and 9.

This type of calorimeter was selected for the forebody because analysis had shown that the high input heat fluxes render film or thin disc types impractical since their useful lifetimes before melting would be extremely small. In addition, the slug calorimeter matches the beryllium shield in thickness and material, thus providing a virtually homogeneous structure. Mating surfaces are machined and honed to microinch accuracy, thereby eliminating thermal interface resistance. These features, coupled with the relatively flat radial variation in heat flux and shield thinness, result in an approximately one-dimensional heat flow pattern. This provides satisfactory analytical accuracy with the available instrumentation.

Four thermocouples record temperature responses at different depths in each calorimeter. These depths are: one at approximately 10 mils beneath the heated surface; one at the rear surface; and two at intermediate points. In addition, as shown on Fig. 2, there is a 200 percent redundancy of thermocouples per location on each shield. Interpolation accuracy between the various readings is therefore improved, a unified, depth-wise temperature response may be synthesized from the redundant readings , and a large measure of safety is provided against malfunction of any particular thermocouple.

The thermocouples are made of premium grade, 1-mil diameter chromel-alumel wire, encased in a double-bore 3.5-mil quartz sheath. Such fine wire gauges were selected in order to gain the advantages of rapid response, negligible conduction heat loss along the wires, minimal disturbance to the homogeneity of the calorimeter slug, and small thermocouple junction size. The first and second advantages are obvious; the third arises from the fact that the 5-mil hole, which is sufficient to contain the insulated thermo-

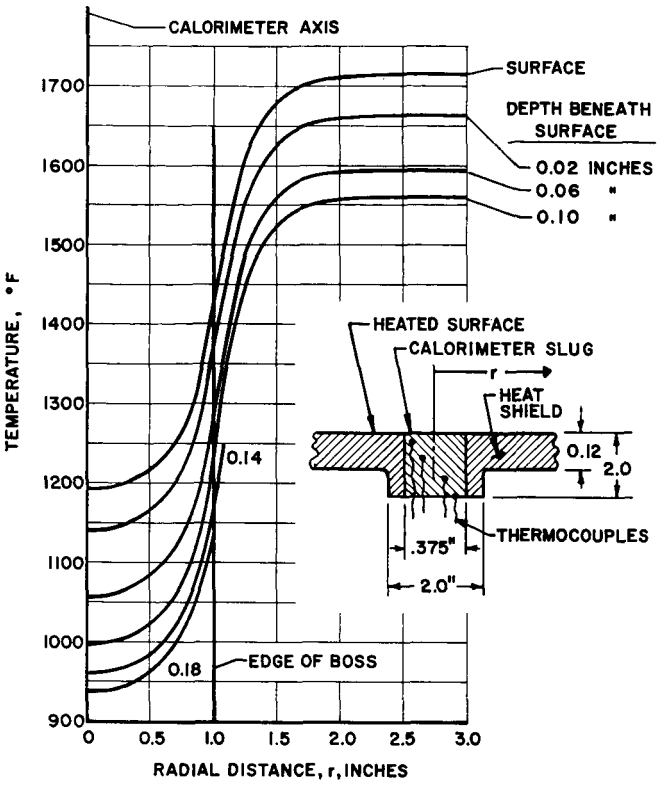

Fig. 9 - Instantaneous time-temperature pattern on first beryllium heat shield boss (2-inch diameter calorimeter boss)

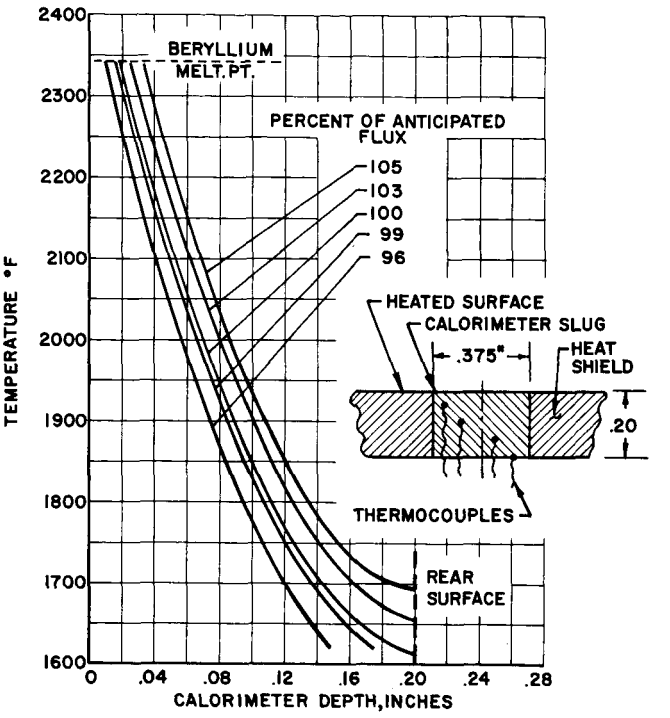

Fig. 10 - Typical calorimeter temperature responses (second beryllium heat shield)

couple, will not cause more than a one percent error in the temperature response. The importance of the small junction size may be deduced from calculated temperature response characteristics as shown in Fig. 10. It is seen that at a time instant near the onset of melting for the second beryllium shield, a very sharp temperature gradient occurs near the heated surface. Here, each mil of depth corresponds to a temperature difference of 7°F. Hence, junctions much larger than the three mil design limit could diminish the accuracy of the temperature readout.

Such fine wire instrumentation also has concomitant disadvantages which should not be minimized. Delicate handling techniques must be employed to avoid breakage and distortion which can alter the EMF characteristics. In addition, to ensure high reliability, the calorimeter assemblies are subjected to qualification tests which apply stress conditions more severe than those anticipated during the various phases of the trajectory.

The middle heat shield is thicker than the inner and outer ones to provide a comparable lifetime despite its more intense heating period. Although the thicknesses of the beryllium shields differ, the calorimeter slugs are all of the same depth, and are interchangeable to facilitate fabrication, installation, and data reduction. This is accomplished, still retaining essentially one-dimensional depthwise heat flow, by providing the thinner shields with bosses to accommodate the full calorimeter length. These boss diameters must be sufficiently large to retain the one-dimensional characteristic of the calorimeter heat flow. Figures 8 and 9 show some typical results of an analysis to determine satisfactory boss diameters. In the case of Fig. 8, the instantaneous local temperature pattern around the thermocouples on the calorimeter axis does not exhibit the flat gradient characteristic of one-dimensional flow. Accordingly, the assumed 1.5-inch boss is too small, since it is influenced by heat flow from the thinner surrounding shell. The instantaneous temperature responses in the 2.0-inch diameter boss of Fig. 9 have the proper flat shape near the calorimeter axis, thus permitting for the purposes of analysis, the assumption of a uniform 0.20-inch cross-sectional thickness.

Possible errors due to calorimeter manufacturing and installation tolerances were also investigated. One of these is the determination of the error resulting from welding the thermocouple junction at a depth differing from its design location. Using Fig. 10 it was found, for instance, that thermocouples nominally 10 mils from the heated surface would indicate absorbed heat fluxes about 1% high for each 3 mils of deeper location. Conversely, locations 3 mils closer to the surface cause a flux error about 1% low. With junctions at greater depths, the error, of course, will be still less than the small amounts noted here. Another error

results when a limiting corner radius is specified for the outboard shoulders of the holes provided in the shields to receive the shrink-fitted calorimeter slugs. Ideally speaking, these corners should be perfectly sharp so that joint lines of mating parts are smooth and do not cause surface irregularities which could increase local convective heating rates or distort the temperature patterns in the vicinity of the instrumentation. An analysis indicated that with the corner radius held to 3 mils (which is the minimum practically achievable) the outboard thermocouple readings in the stagnation area will be high by a constant 20°F during most of the second beryllium shield heating period. This area was selected for analysis since it is subjected to both the highest heat flux and highest rate of change of heat flux. The effects of such a surface discontinuity, therefore, would be most pronounced here.

Further errors, which may be expected in the computed heat flux, result from telemetering system inaccuracies and an inaccurate knowledge of the thermophysical properties of the beryllium heat shield material. These are known within about 5%. The ultimate accuracy of the computed heat flux is a function of the accumulation of all the errors indicated. Accordingly, the necessity for minimizing the numerous sources of calorimeter error can be appreciated.

AFTERBODY CALORIMETER

The afterbody calorimeter design problem is considerably different from that of the forebody since the anticipated heat flux is about 25 times less. It was determined that the optimum type of calorimeter is a thermally isolated, small diameter, relatively thin metal disc of high thermal conductivity. Accordingly, a simple configuration was derived consisting of an 0.45-inch diameter pure gold disc mounted in a low conductivity natural lava stone housing shown schematically in Fig. 11. This housing is flush mounted within the afterbody phenolic-asbestos thermal protection material.

Sensor instrumentation consists of two redundant 10-mil diameter chromel-alumel thermocouples installed in individual holes drilled in the inboard face of the gold. The thermocouples are retained by peening the holes closed over each junction. The two thermocouples will give exactly the same signal since negligible temperature gradients occur in the gold sensor.

The advantages of this design are reliability, sensitive response to anticipated heat flux (Fig. 12), and ease of data reduction. Gold was selected as the sensor material because of its very high thermal conductivity, sufficiently high melting temperature, resistance to oxidation, and well known thermophysical properties. The sensor discs are required

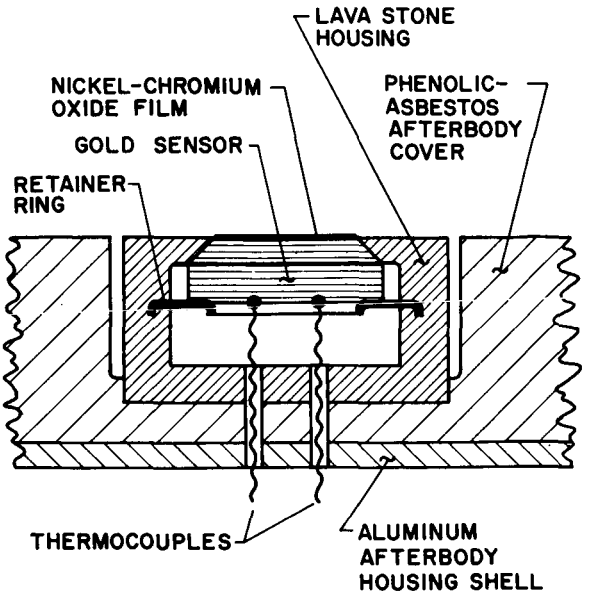

Fig. 11 - Afterbody calorimeter - simplified cross section

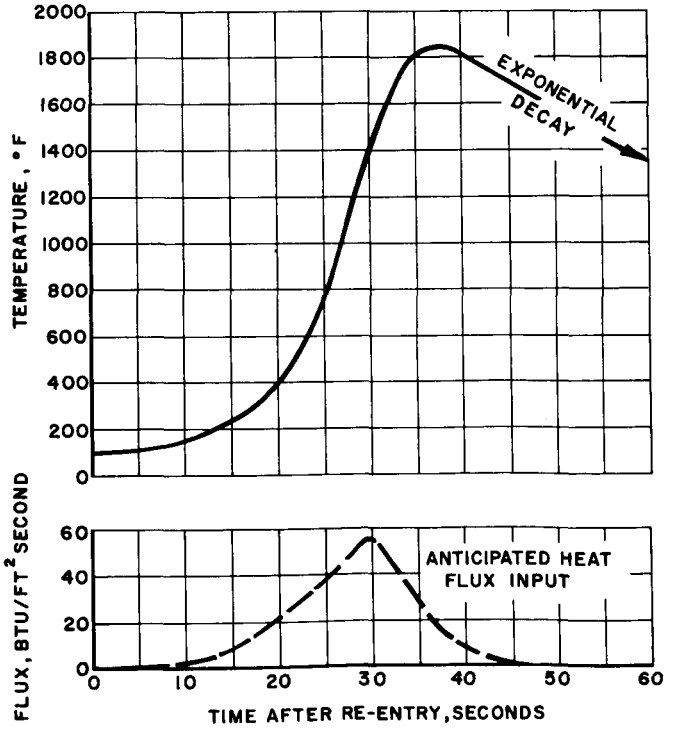

Fig. 12 - Typical afterbody calorimeter temperature response

to be 0.13 inches thick to approximately match temperature responses occurring in the adjacent material. Thus the ever present problem of instrument heat conduction error

is reduced in this local area. Additional heat loss error from the calorimeter disc has been minimized by maintaining a very small contact area between the sensor and its supporting structure. In effect, a void exists between the housing and most of the free gold surface across which heat can only be transferred by radiation. This radiation is limited to a negligible quantity by the very low natural emissivity (approximately equal to 0.04) of the inboard gold surfaces.

The outboard surface of the sensor disc is coated with a carefully calibrated, high-emissivity, nickel-chromium oxide film. This increases the calorimeter sensitivity and serves to maintain the sensor temperature at levels comparable to those of the surrounding lava housing.

The accuracy of the computed heat flux is dependent upon the tolerance to which the nickel-chromium oxide film emissivity is known. Figure 13 indicates the extent of the computed flux error resulting from a deviation in the estimated 0.750 emissivity. It is seen that in the interval when the input heat flux pulse is rising (during the first 30 seconds after re-entry), a 2% accuracy may easily be obtained if the emissivity is known within approximately 20%. However for the 10-second interval beyond the peak, emissivity must be known within 4% if the calculated flux is to be estimated within 8%.

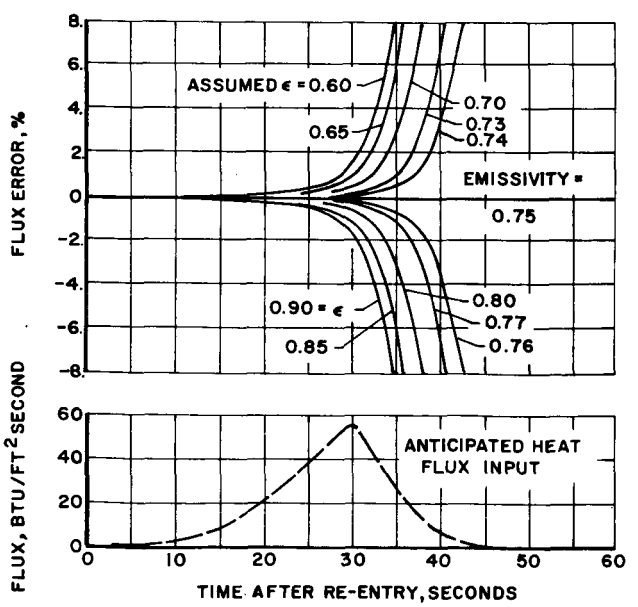

Fig. 13 - Error in calculated emissivity values

DATA ANALYSIS

Reduction of the telemetered temperature data to heat flux values presents interesting mathematical problems which are only briefly considered in this paper. In analyzing the forebody calorimeters it was found convenient to divide the heating period of each shield into two regimes. During the first of these the calorimeters respond as semi-infinite one-dimensional solids, while through out the second regime they react as finite one-dimensional slabs. Closed form temperature inversion equations have been derived by the authors to cover these heating modes. For the initial mode, the semi-infinite solid, the equation is

$$\dot{q}(\theta)=\sqrt{k\rho c\pi}\int_0^{\theta}\left[\frac{\partial T}{\partial \tau}\exp\left(\frac{x^2}{4\alpha(\theta-\tau)}\right)\right]\left[1-\frac{x^2}{4\alpha(\theta-\tau)}\right]d\tau \qquad (1)$$

where $\frac{\partial T}{\partial \tau}$ is the slope of the experimentally determined time-temperature trace at a specific location, x , in the calorimeter. During the second regime, the following equation is valid

$$\dot{q}(\theta)=\frac{\partial Q(\theta)}{\partial \theta}=k\sqrt{\pi}\int_0^{\theta}\frac{\frac{\partial(\Delta T)}{\partial \tau}\left[1-\frac{2L^2}{\alpha(\theta-\tau)}\sum_{-\infty}^{\infty}\left(\frac{x}{2L}-\frac{1}{2}+n\right)^2\right]}{2\sqrt{\theta-\tau}\sum_{n=-\infty}^{\infty}\exp\left\{\frac{-L^2}{\alpha(\theta-\tau)}\left(\frac{x}{2L}-\frac{1}{2}+n\right)^2\right\}}d\tau \qquad (2)$$

where

$$\frac{\partial(\Delta T)}{\partial \tau}=\frac{\partial(T(x,\tau)-T(0,\tau))}{\partial \tau} \qquad (3)$$

and is experimentally determined as the slope of the temperature difference trace with respect to time. The symbols used in these equations are:

- c = Specific heat of the calorimeter material (BTU/lb°F)
- k = Thermal conductivity of the calorimeter material (BTU/sec f^2°F)
- L = Heat shield thickness (ft)
- n = Summation index, integers, 1,2,3,....
- $\dot{q}$ = Heat flux (BTU/f^2 sec)
- $Q(\theta)$ = Total heat flux absorbed between times zero and θ (BTU/f^2)
- T = Measured temperature in calorimeter assuming initial temperature is zero (°F)
- x = Depth within calorimeter (ft)
- α = Thermal diffusivity (ft^2/sec)
- θ = Time (seconds)
- ρ = Density of calorimeter material (lb/f^3)
- τ = Dummy time variable (seconds)

These equations are complex but readily lend themselves to digital computer programming.

Inversion of the afterbody calorimeter temperature

responses to heat flux is relatively simple. As has been mentioned previously, temperature gradients do not occur in the gold discs due to their high thermal conductivity and the moderate heat input. The discs, therefore, act as homogeneous bodies absorbing convective heat on the outboard surface and simultaneously radiating a portion of it to space from the same surface. The instantaneously applied heat flux is, therefore, equal to the sum of the heat quantity that is absorbed by the disc, the heat lost by radiation from its high emissivity surface, and the very small readily estimable heat leakage through the supporting structure. This is expressed as

$$\dot{q} = \frac{wc}{A}\frac{dt}{d\theta} + \sigma\epsilon t^4 + \text{small losses} \qquad (4)$$

in which the additional symbols are:

- A = Calorimeter outboard surface area (ft^2)
- t = Absolute temperature (°R)
- w = Weight of sensor (lb)
- ϵ = Hemispherical emissivity
- σ = Stefan-Boltzmann constant ($BTU/sec\ °R^4 ft^2$)

CLOSURE

A natural follow-on to Project FIRE would be flight testing at re-entry velocities corresponding to planetary return. At 44,000 ft/sec, which is a representative earth re-entry velocity for certain Martial missions, the heat flux to the forebody of the Project FIRE type vehicle varies from 4000 to 8000 $BTU/ft^2 sec$. depending upon the particular $W/C_D A$ and re-entry angle investigated. Such a vehicle, presently under study at the Republic Aviation Corporation Space Systems Division, presents unprecedented difficulties in calorimeter design. However, the experience gained from Project FIRE should be of great value in providing insight towards the solution of these problems of the future.

REFERENCES

1. Kivel, B., and Bailey, K., "Tables of Radiation from High Temperature Air," AVCO-Everett Research Laboratory Report 121, December 1957.

2. Allen, R. A., Rose, P. H., Camm, J. C., "Non-Equilibrium and Equilibrium Radiation at Super-Satellite Re-Entry Velocities," Institute of Aerospace Science Paper 63-77.

ACKNOWLEDGEMENT

The authors wish to acknowledge the many useful discussions with members of the Flight Re-Entry Programs Office of the NASA Langley Research Center, and to express their appreciation to those persons who assisted in the preparation of this paper, particularly the Publications Group at Republic's Research and Development Center and Mr. Peter Zawoiski of the Space Systems Division.

Paper subject to revision. SAE is not responsible for statements or opinions advanced in papers or discussions at its meetings. Discussion will be printed if paper is published in Technical Progress Series, Advances in Engineering, or Transactions. For permission to publish this paper, in full or in part, contact the SAE Publications Division and the authors.